Synthesis and Characterization of Gd doped BSCCO-2212

Thesis Submitted
for the partial fulfilment
of
the Degree of M.Sc. in Physics

Submitted By

Sikha Kanungo
Roll no.-411ph2097

Under the guidance
of
Dr. P. N. Vishwakarma
DEPARTMENT OF PHYSICS

NATIONAL INSTITUTE OF TECHNOLOGY
ROURKELA, MAY 2013

Declaration

I do *hereby declare that the research work incorporated in the thesis entitled* "***Synthesis and Characterization of Gd doped BSCCO-2212***" *is an original research work carried out by me independently in the Department of Physics, NIT Rourkela under the direct supervision and guidance of Dr. P. N. Vishwakarma. The work has not been submitted to any other Institute for any degree.*

Date: **Sikha Kanungo**

ACKNOWLEDGEMENT

I heartily express my deepest sense of gratitude to my supervisor **Dr. P. N. Vishwakarma**, Department of physics, NIT Rourkela for his suggestion and guidance .His great interest, encouragement and guidance had made my work fruitful.

I extend my special thanks to **Jashashree Ray and Achyuta Kumar Biswal**, research scholars Dept. of Physics, NIT Rourkela for their help in thesis work and valuable views throughout my work.

I would also like to thank my labmate **Amrita Singh** and my batchmates for their support throughout the work.

Last but not the least I'd definitely thankful to my **parents and sisters** for their encouragement and support and being great inspiration.

Date: **Sikha kanungo**

Department of Physics
National Institute of Technology Rourkela
Rourkela, Odisha, India -769008

CERTIFICATE

This is to certify that the thesis entitled "***Synthesis and Characterization of Gd doped BSCCO-2212***" being submitted by **Sikha Kanungo** in partial fulfilment of the requirements for the award of the degree of Master of Science in Physics at National Institute of Technology, Rourkela is an authentic experimental work carried out by her under our supervision. To the best of our knowledge, the experimental matter embodied in the thesis has not been submitted to any other University/Institute for the award of any degree or diploma.

***Dr. P. N.* Vishwakarma**
Department of Physics
National Institute of Technology
Rourkela, 769008

Date:
Place: Rourkela

ABSTRACT

Since the discovery of High Temperature Superconductivity in cuprates such as YBCO and BSCCO, researches has been carried out on flux pinning in these materials in order to find ways of increasing their critical current density J_c for practical applications. In order to prevent vortex motion, vortices must be pinned against increasing magnetic field or current density. Several methods have been reported, for instant, adding nanosize impurity phases to the superconductor like YBCO, columnar defects generated by ion irradiation, point defect generated by oxygen deficiency, chemical substitution or by doping with magnetic nano particles (to avoid hysteresis). In this report the magnetic doping is done at Cu site of BSCCO, so that the dopant forms strong bond within the BSCCO structure, which prevents its motion and thereby preventing vortex motion. Specifically Gd doping with different concentrations such as 1%, 3% and 5% are done and their characterization are also done by various methods like x-ray diffraction, scanning electron microscope, temperature dependence of resistivity, current (I) – voltage (V) measurement. Effect of doping on the value of J_c is analyzed.

CONTENTS

List of Figures

CHAPTER-1

An Overview of Superconductivity and High T_c Superconductors.

1.1 INTRODUCTION

At very low temperatures, the electric and magnetic properties of some materials called superconductors change and they show zero electrical resistance and expel all the magnetic fields. This condition of zero resistivity or infinite conductivity can only be achieved when the metal or alloy is cooled below a certain temperature called critical temperature. This zero resistivity or infinite conductivity is known as superconductivity. In the superconducting state, these materials have the ability to transport large DC currents with no measurable resistive losses. To do this, a superconductor must be kept below three critical parameters, critical temperature (T_c), critical field (H_c), and critical current density (J_c).

With the advent of superconductors having Tc more than boiling point of liquid nitrogen (hence called high Tc superconductors or HTS), a new gateway is opened for various applications, which otherwise was limited for low Tc superconductors. Unfortunately, the current density in HTS materials decreases dramatically with increasing temperature. In addition, to achieve high current densities in HTS materials, either a complicated processing route (YBCO) or an expensive sheath material (BSCCO) is needed. There are many applications of superconductor such as transmission of power, switching devices, sensitive electrical instruments, memory/storage element in computers, manufacture of electrical generators and transformers, nuclear magnetic resonance (NMR).

The most common HTS materials of choice are YBCO and BSCCO. YBCO however suffers from a loss of oxygen and fast degradation in air. Bi based superconductors in contrast are rather stable with respect to oxygen losses. In HTS small coherence length and large penetration depth lead to relatively low pinning energies.

The study of the effect of impurities on the physical properties of superconductors is of great importance. In conventional superconductors, nonmagnetic dopants cause changes in superconducting transition temperature and changes in electron density or the removal of anisotropies in pair coupling. The destructive effect of doping in HTS has been disappointing from a purely technological point of view because doping has neither led to enhancement of T_c nor improvement in quantities such as critical current. The microstructural and electrical homogeneity of BSCCO 2212 provides a good basis to study of effects of doping. Impurity substituted on Cu sites in HTS generally is found to cause rapid suppression of the

superconducting transition temperature. The limitations from flux pinning at elevated temperature for BSCCO 2212 gained interest for increase in flux pinning in BSCCO 2212.

1.2. A brief History about High T_c superconductor

In the year 1986 for the first time superconductivity was observed in oxides ($La_{2-x}Ba_xCaO4$) with T_c as high as 30K. After this many oxide based superconductors were discovered with much higher T_c and J_c. This opened a new branch of high T_c superconductivity as they broke the barrier of 30K imposed by BCS Theory.

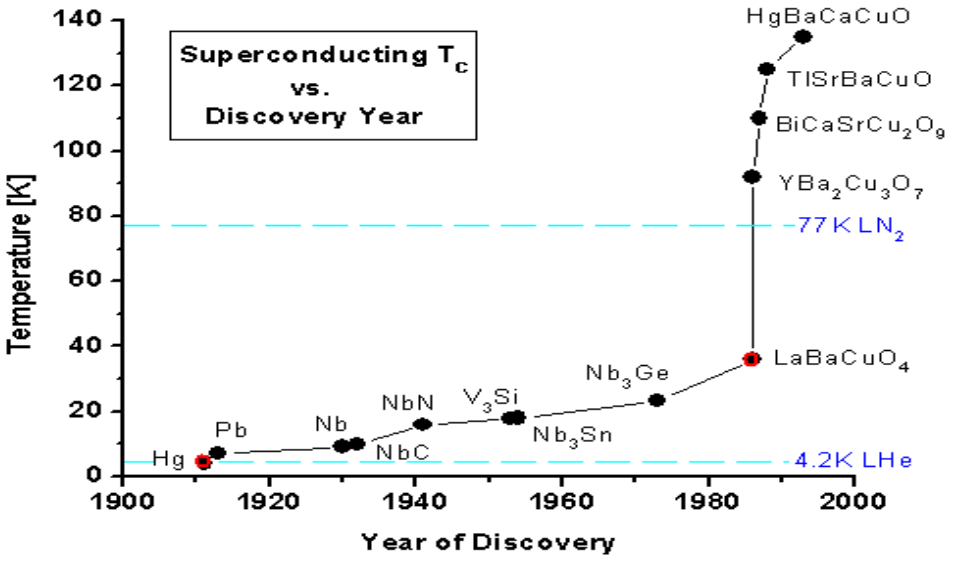

Fig 1. Superconducting T_c Versus Discovery year

Following are some known high T_c Superconductors of this family.

- LBCO: LBCO [$(La,Ba)_2CuO_4$] is the first oxide based HTS material having T_c equal to 35K. It is the only insulating material In the HTS family.
- YBCO: YBCO (YBa2Cu3O7-x) is the first material to break liquid nitrogen temperature. Highest Tc achieved by YBCO system is around 90K.
- BSCCO: General formula of BSCCO system is $Bi_2Sr_2Ca_{n-1}Cu_nO_{2n+4}$ with specific transition temperature ranging from T_C = 20K (n = 1, 2201 phase), 85K (n = 2, 2212 phase) and 110K (n = 3, 2223 phase).

- TBCCO: General formula $Ti_2Ba_2Ca_{n-1}Cu_nO_{2n+4}$ with specific transition temperature ranging from TC=85K (n = 1, 2201 phase), 110K (n = 2, 2212 phase) and 125K (n = 3, 2223 phase).

1.3. SOME PROPERTIES OF SUPERCONDUCTOR

1.3.1. Zero Resistivity

In a superconductor, below a temperature called the "critical temperature", the electric resistance very suddenly falls to zero. At zero resistance, the material conducts current perfectly. Above T_c superconductors exhibit ohmic conductivity, as for a normal metal. At and below T_c, in the absence of a magnetic field, resistivity falls to zero.

We can study the nature of superconductivity using "free electron model". The resistivity of a metal may be written as,

$$\rho = m/ (ne^2\tau)$$

where : m- mass of an electron

n- no. of electrons

e- electronic charge

τ- relaxation time

The decrease in temperature is followed by the freezing of lattice vibration and hence the scattering of electron diminishes. This results in a longer τ i.e. the time taken between the collision of two electrons is more and hence a smaller ρ.

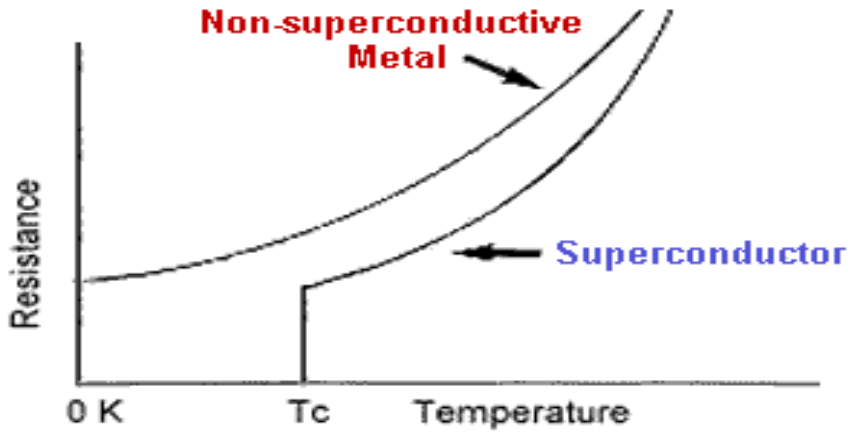

Fig.2 Resistance vs Temperature for Superconducting and non-superconducting materials

1.3.2 Meissner Effect And Perfect Diamagnetism

In 1933, two physicist, Meissner and Ochsenfeld, observed that a superconductor expels magnetic flux completely, a phenomena known as Meissner Effect. According to this effect, as the temperature is lowered to T_c, the flux is suddenly and completely expelled as the specimen becomes superconducting. Further it's been observed that this effect is reversible.

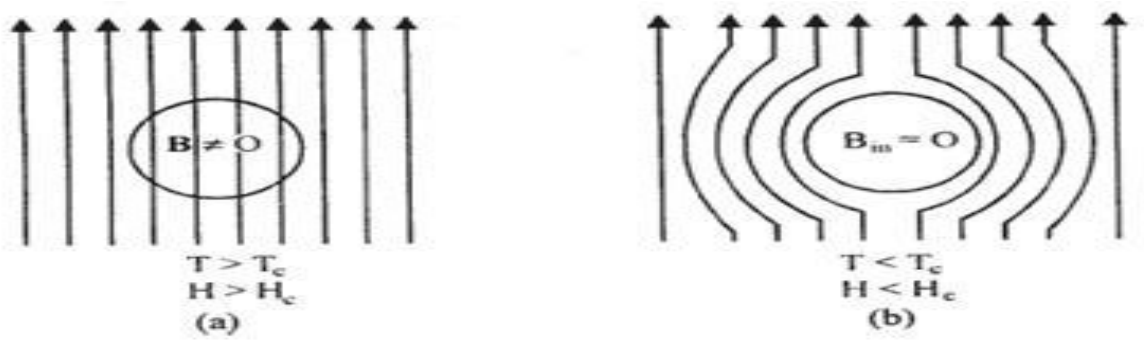

Fig.3 Meissner Effect for Normal conductor and superconductor showing the allowance of magnetic flux in case of normal conductor whereas complete exclusion of the same while it becomes superconductor.

Since B=0 in the superconducting state, it follows that

$$B = \mu_0 (H+M) \qquad \text{i.e. } 0 = \mu_0 (H+M)$$

$$\text{or, } H = -M \qquad \text{or, } \chi = -1$$

Where, H = strength of the field, M = magnetization or intensity of magnetization, χ is susceptibility of the material

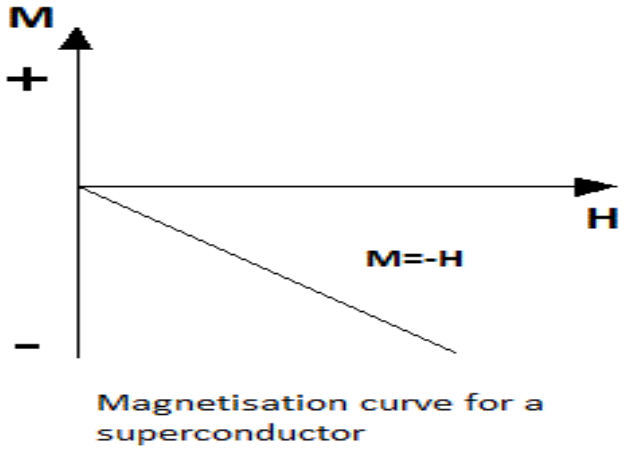

Fig.4 Magnetization curve for superconductor

1.3.3. Critical field:

Superconductivity can be destroyed by the application of magnetic field. If a strong enough magnetic field, called critical field, is applied to a superconducting specimen, it becomes normal and recovers its normal resistivity even at $T<T_C$.

The critical field depends on the temperature. For a given substance, the field decreases as the temperature rises from T=0 K to $T=T_c$. It has been found empirically that the variation is represented by

$$H_c(T) = H_c(0)[1-(T/T_c)^2]$$

Here, Hc (T) = maximum critical field strength at temperature T.,
Hc (0) = maximum critical field strength occurring at absolute zero.

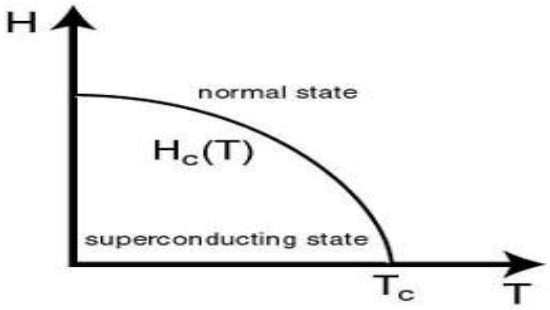

Fig.5. Critical field vs Temperature for superconductors

1.3.4. Transition Temperature or Critical Temperature (T_C):

Temperature at which a normal conductor loses its resistivity and becomes a superconductor, is known as the transition temperature or critical temperature. It is definite for a material. Superconducting transition is reversible.

1.3.5. Magnetic Flux Quantization:

Magnetic flux enclosed in a superconducting ring = integral multiples of fluxon

$\Phi = nh/2e = n\,\Phi_0$ $\qquad$ $(\Phi_0 = 2x10^{-15}Wb)$

1.3.6 Critical Current density:

It is the maximum electrical transport current density that the superconductor is able to maintain without resistance. This critical value was temperature dependent, increasing as the temperature was reduced below the critical temperature, according to the expression

$$J_c(T)=J_c(0)(T_c-T)/T_c$$

1.4 TYPES OF SUPERCONDUCTOR

1.4.1. Type I Superconductor

Type I superconductors are those superconductors which lose their superconductivity very easily or when placed in the external magnetic field. From the graph of magnetization (M) vs applied magnetic field (H), when the type I superconductor is placed in the magnetic field, it suddenly loses its superconductivity at critical magnetic field (H_c).These are hard superconductors.

1.4.2. Type II Superconductor

Type-II superconductors are those superconductors which lose their superconductivity gradually but not abruptly when placed in the external magnetic field. From the graph of intensity of magnetization (M) versus applied magnetic field (H), when the type-II superconductor is placed in the magnetic field, it gradually loses its superconductivity. Type-II superconductors start to lose their superconductivity at lower critical magnetic field (H_{c1}) and completely lose their superconductivity at upper critical magnetic field (H_{c2}). These are soft superconductors.

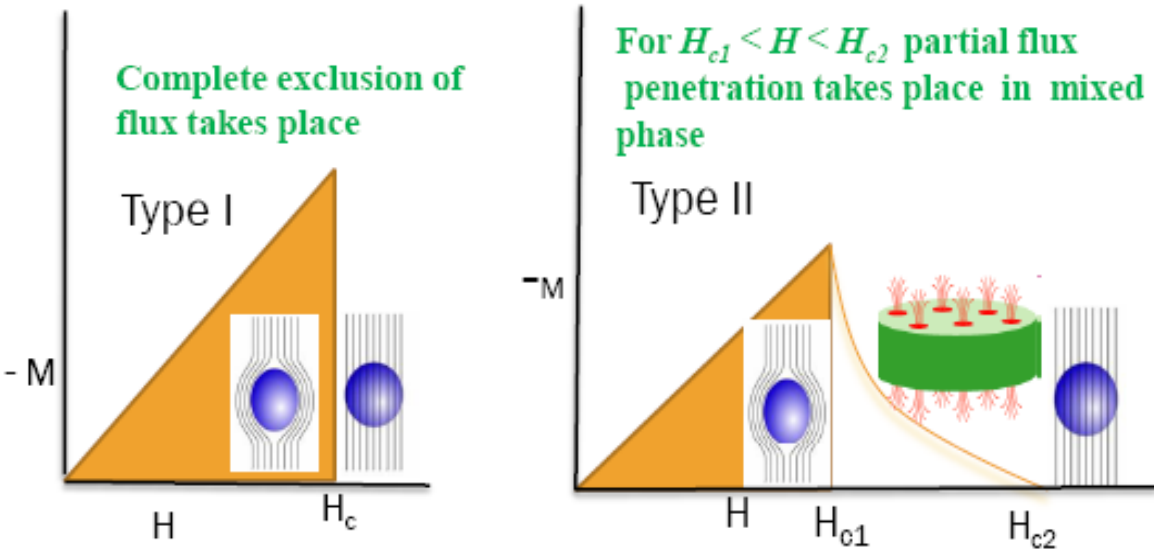

Fig.6. Type-I and Type-II superconductor

1.5. Flux Lattice:

A configuration created when flux lines from a strong magnetic field try to penetrate the surface of a type II superconductor. The tiny magnetic moments within each resulting vortex repel each other and a periodic lattice results as they array themselves in an orderly manner.

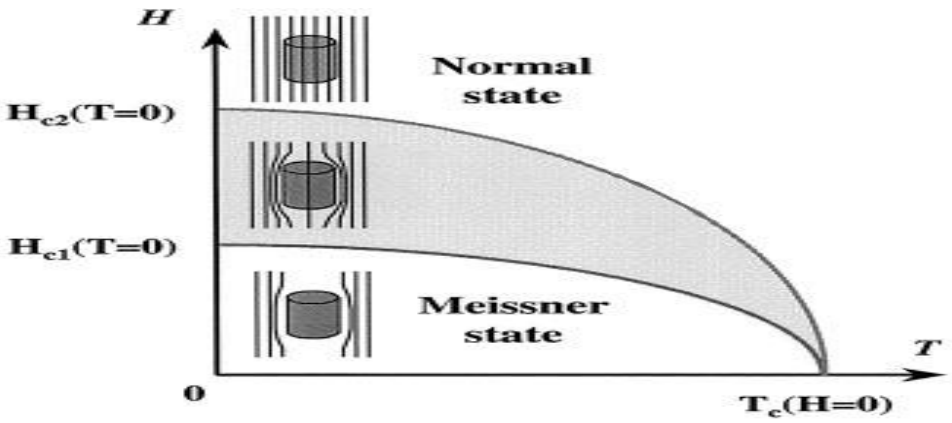

Fig.7 Field penetration for type-II superconductor

1.6. Flux Flow and Pinning:

The phenomenon where a magnet's lines of force (called flux) become trapped or "pinned" inside a superconducting material. This pinning binds the superconductor to the magnet at a fixed distance. Flux-pinning is only possible when there are defects in the crystalline structure of the superconductor (usually resulting from grain boundaries or impurities). Flux-pinning is desirable in high-temperature ceramic superconductors in order to prevent "flux-creep", which can create a pseudo-resistance and depress J_c and H_c. Swirling tubes of electrical current induced by an external magnetic field into the surface of a superconducting material that represent a Type II superconductors during "mixed-state" behavior when the surface is just partially superconducting are the vortex(flux). Flux lines in the mixed state tend to move when high magnetic field is applied due to the increasing Lorentz force.

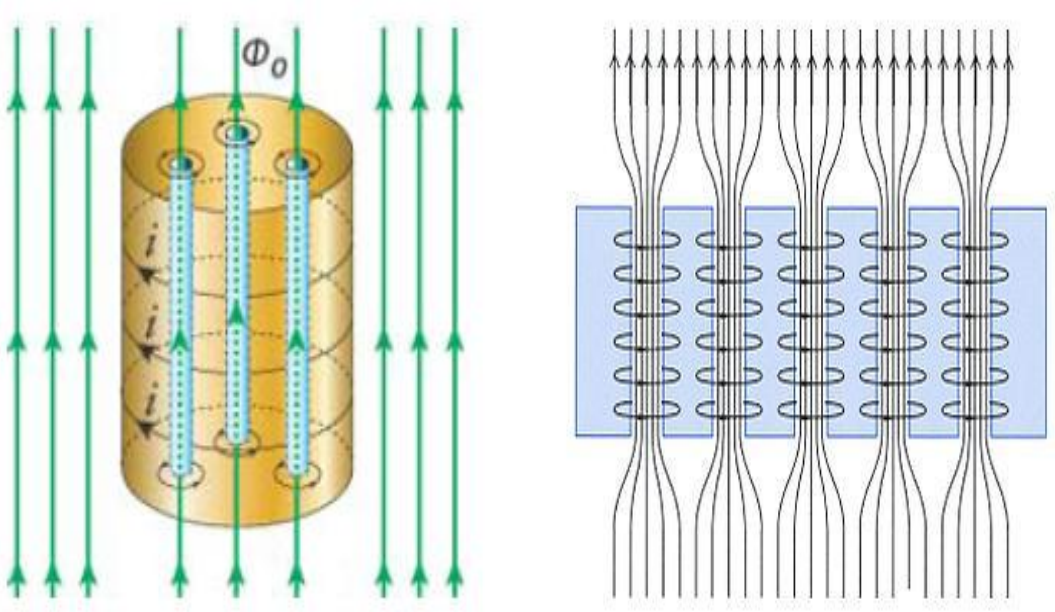

Fig.8 Vortex and Vortex motion in type II superconductor

1.7. BCS THEORY:

In 1957, Bardeen, Cooper and Schrieffer (BCS) proposed a theory that explained the microscopic origins of superconductivity, and could quantitatively predict the properties of superconductors. Cooper (1956) showed that the infinite conductivity in superconductors is achieved due to the formation of pairs of electrons. These pairs are known as ***Cooper pairs***

and are formed by electron-electron interaction. Suppose two electrons lie just inside the Fermi surface and repel each other because of the Coulomb interaction. But this coulomb force is reduced on account of the screening due to the presence of other electrons in the Fermi sphere. So the repulsive interaction between the electrons vanishes. Then due to the interaction between the electrons with lattice points, the two electrons attract each other. Cooper showed that they form a bound state and are paired. This is how cooper pairs are formed which carries super current.

1.8. Joshephson effect

A Josephson junction is made up of two superconductors, separated by a nonsuperconducting layer. The layer acts as a potential barrier, but as it is thin it does not completely inhibit the flow of electrons. The flow of current between the superconductors in the absence of an applied voltage is called a Josephson current, the movement of electrons across the barrier is known as Josephson tunneling. When voltage is applied, a current flows between superconductors by tunneling effect. Quantum tunneling occurs when a particle moves through a space in a manner forbidden by classical physics, due to the potential barrier involved.

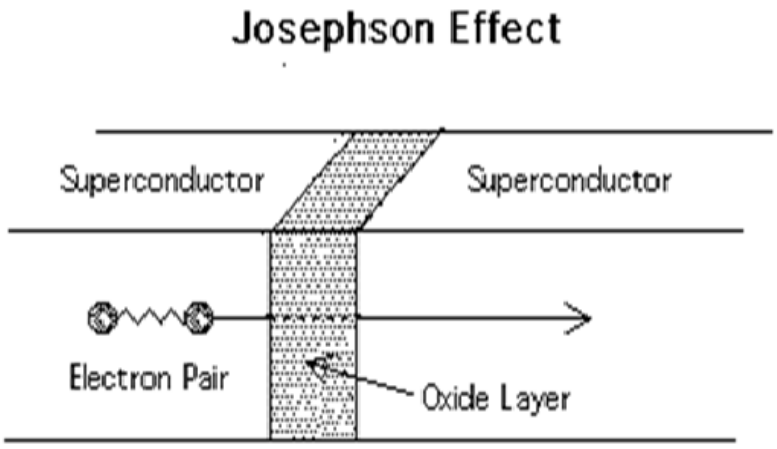

Fig.9 Joshephson Junction

The tunneling which involves cooper pairs, responsible for the Josephson effect. The effect of film is to introduce a phase difference between the two parts of the wave function on opposite

sides of the junction. Numerically Joshephson frequency falls in the microwave range. Usually it is of the order of several milivolts.

1.9.Literature Survey :

D. H. Galvan, A. Durán, F. F. Castillon, E. Adem, R. Escudero, D. Ferrer, A. Torres, J. supercond. Nov Magn, **21**, 271-277 (2008):

Here polycrystalline BSCCO with carbon nanotubes were synthesized by solid state reaction method and their characterization is done. The critical temperature for the compound is 85K. It's been found that there is an enhancement of 1.42 times the original value of J_c from the pure BSCCO (at 4K) by the inclusion of nanotubes.

Snezhko, Alexey; Prozorov, Tanya; Prozorov, Ruslan, Physical Review B, **71**, 024527 (2005):

Here enhancement of vortex pinning is done by magnetic nano particles embedded into the bulk of type II superconductor studied both theoretically and experimentally. Calculations were made on MgB_2 superconductor with embedded magnetic Fe_2O_3 nanoparticles and compared with MgB_2 with non magnetic Mo_2O_5 pinning centers of similar concentration and particle size distribution. It is shown that ferromagnetic nanoparticles results in a considerable enhancement of vortex pinning in type II SC.

D R Mishra, Pramana journal of physics, Indian academy of sciences, **70**, 535-541 (2008):

The effect of Gd doping at Calcium site on the normal and superconducting properties of Bi 2223 system were studied. The T_c values on comparison with reported values for (BiPb)-2212 specimen suggest that BiPb)-2223 is the main phase responsible for superconductivity upto Gd concentration x>0.8. Gd ,a magnetic impurity contributes towards the pair breaking effects and lowers T_c.

S. Vinu, P.V. Shabana, R. Shabnam, A. Biju, P. Guruswamy,U. Syamaprasad, Solid State Sciences **104,** 043905 (2008):

Gd doped BSCCO with different concentrations were prepared by solid state synthesis in bulk polycrystalline form were studied. The critical current density and flux pinning properties of the system were investigated. The critical temperature T_c, J_c, pinning potential

and flux pinning strength were highly enhanced for samples with concentration 0.2-0.3.The enhancement of J_c and T_c is attributed to the optimization of hole concentration and the formation of point defects due to the doping of Gd atoms at the Sr sites, which acts as flux pinning centers.

1.10. WHY BSCCO

The BSCCO compounds whose superconductivity was first reported by H. Maeda et al., are one of the most important families of high temperature superconductor with technological relevance. They are highly anisotropic layered ceramics with a structure of perovskite crystals, in which the presence of CuO_2 planes, usually set as a-b planes, is essential for superconductivity.

The general formula for Bi-based HTSCs can be stated as $Bi_2Sr_2Ca_{n-1}Cu_2O_{2n+4}$. n can take (n= 1, 2, 3) values for the different number of Cu-O planes perpendicular to the c-axis. Precisely the fact that the current mainly flows in the direction perpendicular to the c-axis makes to require complex fabrication techniques, and their critical current density J_c is heavily dependent on the processing. The fabrication methods are in continuous development and now-a-days BSCCO based materials are achieved in wide range of shapes (thin and thick films, tapes, wires, bars, tubes, etc.)

BSCCO is the important category of high temperature superconductors which did not contain rare earth element and shares a two dimensional layered (perovskite) structure where the superconducting phenomenon varies in copper oxide plane. It gives the high T_c value and shows more stability in superconducting behaviour with respect to oxygen loss in comparison to YBCO. BSCCO compounds exhibit both an intrinsic Josephson effect and anisotropic (dimensional) behaviour. BSCCO is generally categorized into three different structures according to their ‘n’ values. There are, T_c=20K (n=1, 2201), T_c=95K (n=2, 2212). Its T_c is considerably high and it is easy to synthesis as they are thermodynamically stable over a wide range of temperature and within the stoichiometric range, as compared to 2223 phase. For synthesis of 2212 and 2223 phase there require doping with lead. But 2212 phase is the only to be obtained without lead addition.

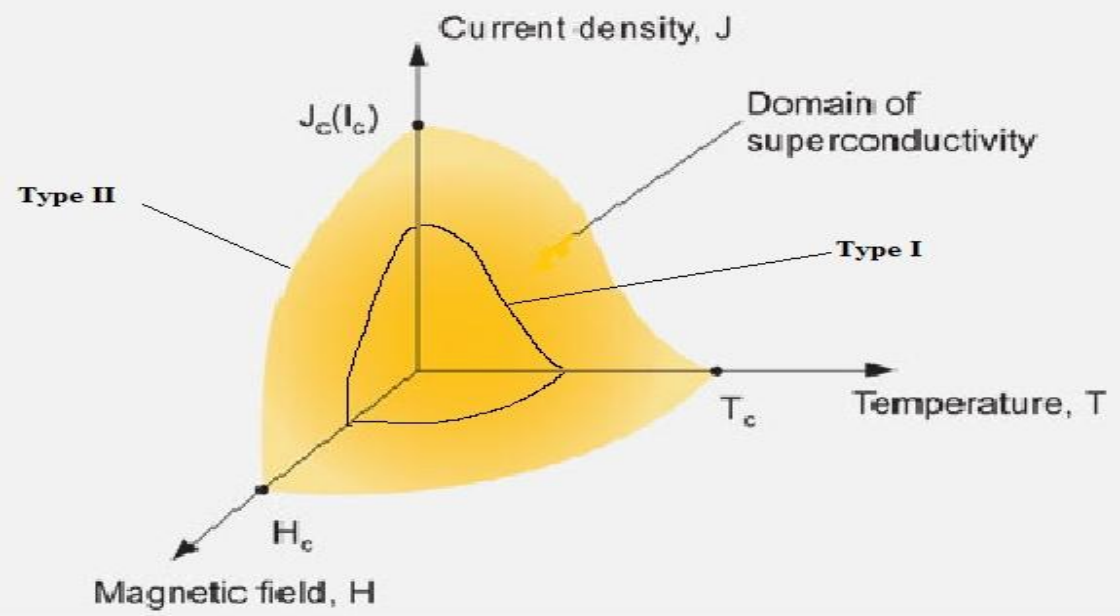

Fig.10 J_c vs H_c vs T_c curve for Type-I and Type-II superconductor

The J_c versus T_c versus H_c graph for type I and Type II superconductor shows that the values of J_c, T_c and H_c are way greater in case of type II in comparison with Type I.

1.11. Why doping is needed in BSCCO?

Since the discovery of HTS in the cuprates such as YBCO and BSCCO, researches has been carried out on flux pinning in these materials in order to find ways of increasing their critical current density J_c for practical applications. To avoid the flux flow i.e. vortex motion in the superconducting sample it's needed to pin this by some means. For HTS vortices experience Lorentz force, hence starts to move. This motion creates an electric field parallel to the current. This results in a finite resistivity $\rho=E/J$, hence energy dissipation. In order to prevent this, vortices should be pinned which will favour the increase of critical current density. Several methods had been reported in the literature in favour of this for instant, adding impurity phases to the superconductor like YBCO, columnar defects generated by ion irradiation, point defect generated by oxygen deficiency, chemical substitution or by doping with magnetic nano particles(to avoid hysteresis).

Here the doping is done in Cu site of BSCCO, so that the dopant forms strong bond within the BSCCO structure, which prevents its motion and thereby preventing vortex motion.

1.12. Crystal Structure of BSCCO

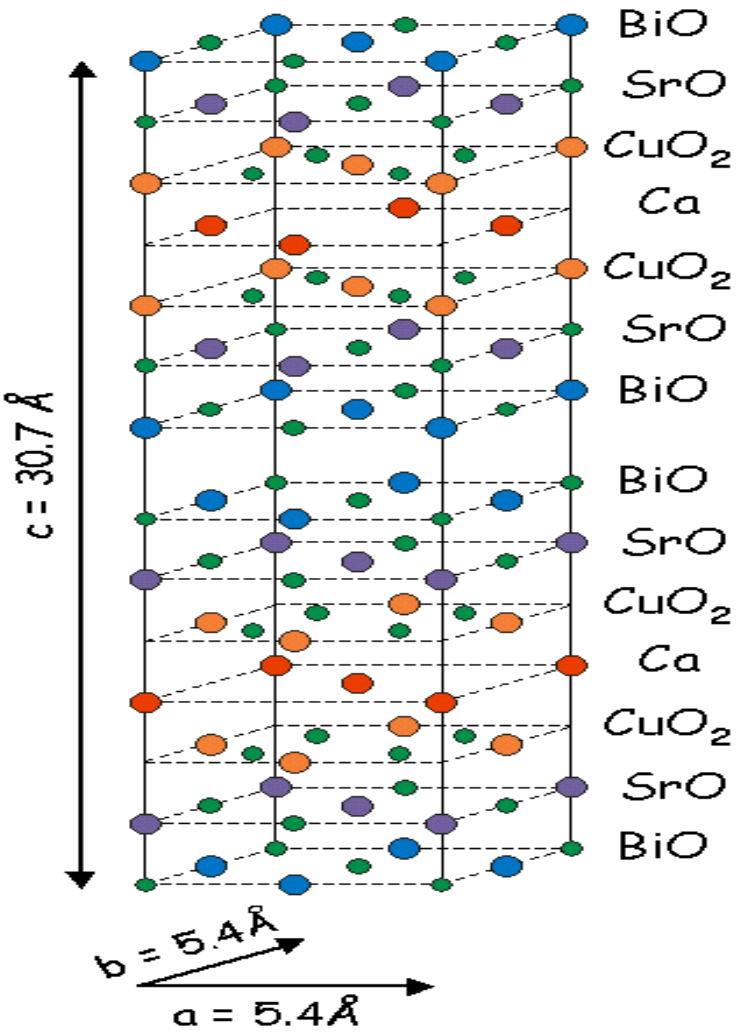

Fig.11. Crystal structure of BSCCO

BSCCO 2212 refers to the formula $Bi_2Sr_2Ca_nCu_{n+1}O_{6+2n}$,where n is an integer. For n=1, it is $Bi_2Sr_2Ca_1Cu_2O_8$(BSCCO). Unit cell of BSCCO structure contains three layers. They are "Reservoir layer"(i.e. SrO and BiO layer) that reserves the electron ,just above it contains superconducting layer(i.e. CuO)in this layer the doping can be possible to vary the property of the superconductors , above this it contains Insulating layer of Ca which provides scope for the formation of Joshephson junction.

CHAPTER-2

Synthesis Technique and characterization methods

2.1. Experimental Techniques & Sample Preparation

There are different ways to fabricate superconducting BSCCO powder starting from raw powders. Amongst these methods, solid state synthesis is most effective due to the simplicity and reduced infrastructure required for this method although other techniques as co-precipitation, pyrolysis or sol-gel are also used. This method involves the mixing of oxides, peroxides, carbonates, or nitrites of Bi, Sr, Cu and Ca. These powders are reacted at elevated temperatures where no melting occurs when pellets of this powder mix are kept. These steps are repeated until the reaction is complete.

2.2. Solid State Reaction Route:

Solid state reaction method is the most frequently used method for the preparation of BSCCO samples. Precursors oxide powders are palletized and then sintered (heat treatment below the melting temperature) to get high T_c phase. The heat treatment cycle can be varied over a temperature range and duration.

2.3. Precursors:

This method involves the mixing of oxides, peroxides, carbonates, or nitrites of Bi, Sr, Cu and Ca. Here the precursors $CaCO_3$, $SrCO_3$, Bi_2O_3 and CuO with 99% purity were taken as starting material.

2.4. Weighing:

The precursors were carefully weighed with accuracy using balance. Stoichiometric amount of ingredients are weighted, mixed thoroughly and ground in an agate mortar and pestle.

2.5. Agate Mortar and pestle:

After mixing of powders it was grinded in the Agate mortar and pestle. During heat treatments intermediate grindings are necessary for uniformity and to reduce the particle size. Agate mortar and pestle are used to grind the solid into fine powders but under conditions that are highly controlled and to minimize the contamination.

2.6. Calcination:

The heating of the mixture not only depends on the form of reactants but also its reactivity. Calcination is used to achieve the desired crystal phase and particle size. For the heating of material high melting point container is used i.e. alumina crucibles (Al_2O_3). Then the mixture is calcined in three stages at temperatures 700 ^{0}C for 12 hr, 770 ^{0}C for 12 hr and 820 ^{0}C for 20 hr in a silicon carbide programmable muffle furnace with a heating rate of 5^0 C/min. Intermediate grinding is done at the end of each heating cycle.

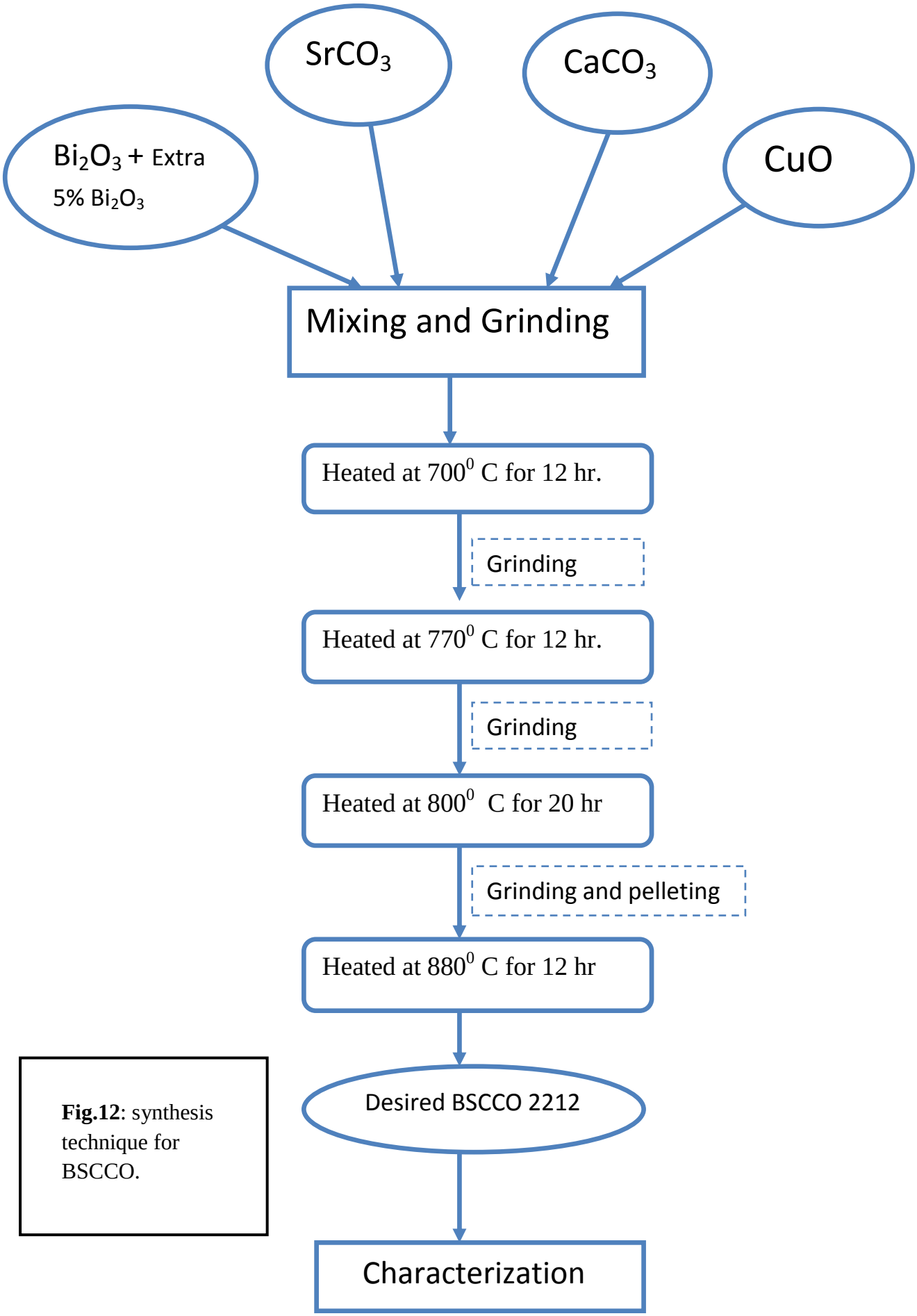

Fig.12: synthesis technique for BSCCO.

[18]

2.7. Method of preparation of BSCCO-2212:

Single phase BSCCO synthesis is the highlight of the research work. Methods of preparation for BSCCO, i.e. solid state synthesis route, melt process, pyrolysis and sol-gel synthesis route, liquid phase technique. Solid state reaction route method is well appreciated for a large-scale production of layered structure. It requires low cost precursors which are readily available.

- The precursors $CaCO_3$, $SrCO_3$, Bi_2O_3 and CuO with 99% purity were taken as starting material. They are mixed in the stoichiometric ratio.
- There is extra 5% Bi_2O_3 is taken to maintain stoichiometry, even in the case of Bismuth loss due to its high vapour pressure.
- The starting precursors and mixed in appropriate amount and then grinded using agate Mortar and pestle and calcined in a programmable electric furnace for 12 hrs at 700^oC.
- After the cooling of the sample grinding with mortar pestle is followed by calcination in furnace for 12 hrs at 770^oC.
- For the third stage of heating again after cooling and grinding, the sample is calcined in the electric furnace for 20 hrs at 820^oC at a heating rate of 5^0C/min.
- After the third heat treatment, the samples are allowed to cool under normal cooling rate and pelletized in a cylindrical die of 10 mm diameter under 5 Kg/cm^2 pressure. Then the pellets are subjected to final heat treatment at 880 ^0C for 12 hr.
- Then various characterizations are carried of the prepared sample.

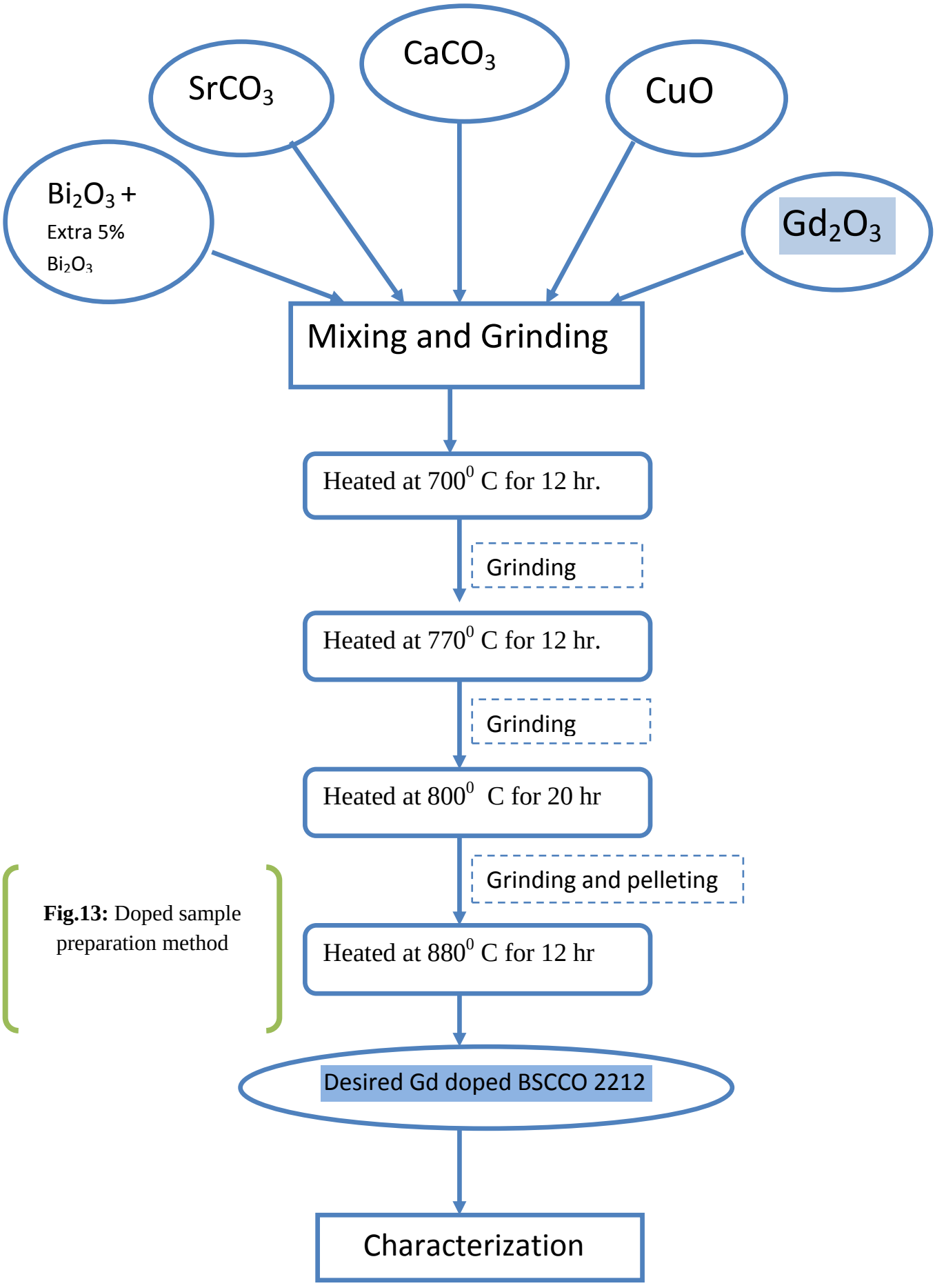

Fig.13: Doped sample preparation method

[20]

2.8.Method of preparation of doped sample:

The appropriate amounts of powdered $CaCO_3$, $SrCO_3$, Bi_2O_3 and CuO and Gd_2O_3 in the stoichiometric ratios of $Bi_2Sr_2Ca\ Gd_x\ Cu_{2-x}O_8$ (x stands for different concentrations) are taken and grinded manually using agate mortar and pestle. Then the same procedure for BSCCO preparation is repeated. $Bi_2Sr_2Ca\ Gd_x\ Cu_{2-x}O_8$ is prepared by same standard solid state reaction. It is just the case different concentrations of doping can be done repeating the same procedure.

2.9. Characterization Techniques

2.9.1. Resistivity Measurement Method (Four Probe Method)

The resistivity is determined by measuring resistance R and the dimension of the sample. From these measurements the resistivity is calculated as

$$\rho = \frac{R \times A}{l}$$

The resistance R is usually determined by a voltage current method. A current value is fed into the sample and the voltage V is measured via point contact. The resistance is then calculated according to Ohm's law. This resistance measurement is done by four probe method.

The advantage of the four probe method over two probe method that it minimizes the other contributions. i.e., lead resistance, contact resistance, etc. to the resistance measurement, which results an accurate measurement of sample resistance. In this method four equally spaced probes are in contact with a material of unknown resistance. The outer two probes are used for sourcing the current and two inner probers are used for measuring the resulting voltage drop across the surface of the sample.

2.9.2 Van der Pauw Method

The theoretical foundation of Hall measurement evaluation for irregularly shaped samples is based on conformal mapping developed by Van der Pauw. He showed how the resistivity, carrier density and mobility of a flat sample of arbitrary shape can be determined without knowing the current pattern if the following conditions are met: the contacts are at circumference of sample and are sufficiently small, the sample is uniformly thick, and does not contain isolated holes.

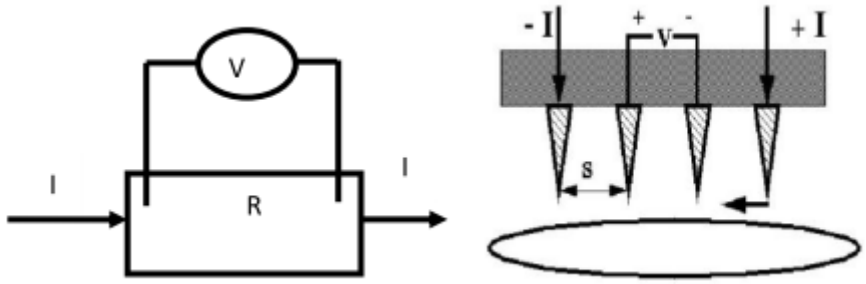

Fig.14 Four probe arrangement

For samples of irregular shape and size, the above two methods may not work, so another methods i.e. Vander Pauw method is followed. This method is commonly used technique to measure the sheet resistance of a material. This consists of two measurements of resistance,

R_A and R_B.

$$R_A = V_{43}/I_{12}$$

$$R_B = V_{23}/I_{14}$$

From these two measurements and from the thickness of the sample under test, the conductivity can be determined by the solution of the equation

$$e^{-\pi RA/Rs} + e^{-\pi RB/Rs} = 1$$

Where R_s is the resistance to be determined.

If R_A and R_B are similar then the above equation be solved for the resistivity as

$$\rho = (\pi d / \ln 2)\ ((R_A + R_B)/2)$$

Where d is thickness of the sample. The precession of such a Vander pauw measurements depends on the flatness and parallelism of the surface of the surface of the sample and on the fact that the contacts are point contacts. Again if R_A and R_B are not similar, then expression for resistivity modifies to

$$\rho = (\pi d/\ln 2)((R_A+R_B)/2)\, f\,(R_A/R_B) \qquad (2.13)$$

where $f\,(R_A/R_B)$ is the function of the ratio of R_A/R_B only.

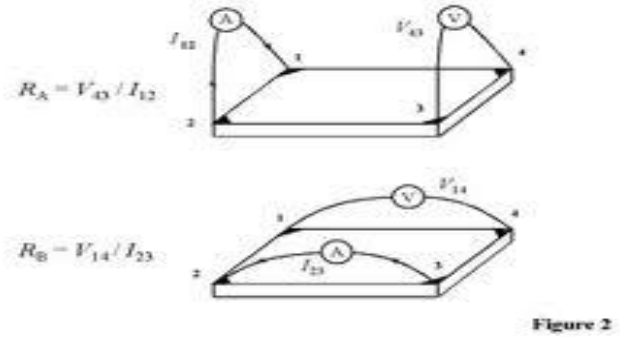

Figure 2

Fig.15 Contacts made in Vander Pauw Method

2.9.3. I-V Measurement(Current- Voltage characteristics)

Current(I)-Voltage(V) measurement is done by varying current and consequently measuring the voltage by nanovoltmeter.

From the current vs voltage plot critical current I_c is found out which when divided by the area of the sample gives the critical current density value.

2.9.4. X-Ray diffraction:

X-ray diffraction (XRD) is an analytical technique looking at X-ray scattering from crystalline materials. Each material produces a unique X-ray "fingerprint" of X-ray intensity versus scattering angle that is characteristic of it's crystalline atomic structure.

When X rays are scattered from a crystal lattice, peaks of scattered intensity are observed which correspond to the following conditions.

- The angle of incidence is equal to angle of scattering
- The path length difference is equal to an integer number of wavelengths .

Bragg's Law of X ray diffraction

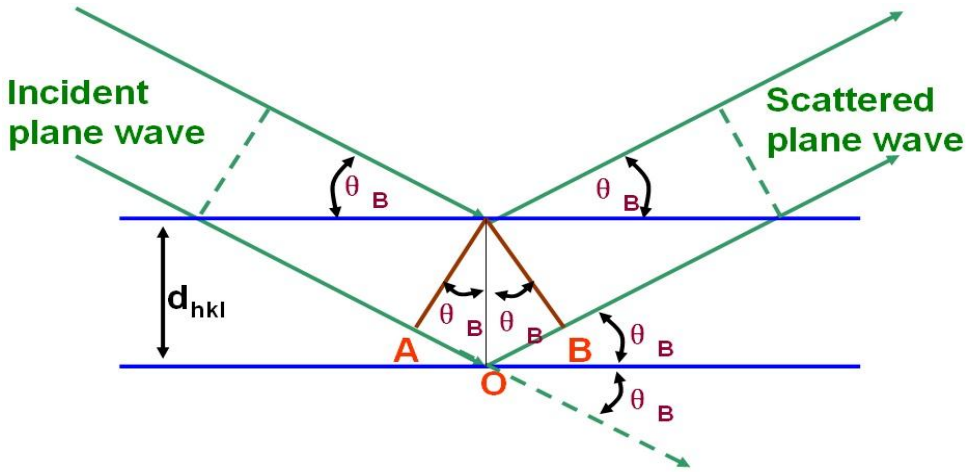

Fig.16 X-ray diffraction

Bragg diffraction occurs when electromagnetic radiation with wavelength comparable to atomic spacings are incident upon a crystalline sample, are scattered by the atoms in the system, and undergo constructive interference in accordance to Bragg's law. For a crystalline solid, the waves are scattered from lattice planes separated by the interplanar distance *d*. Where the scattered waves interfere constructively, they remain in phase since the path length of each wave is equal to an integer multiple of the wavelength. The path difference between two waves undergoing constructive interference is given by $2d\sin\theta$, where θ is the scattering angle.

This can be written as

$$2d\sin\theta = n\lambda$$

Where λ: the wavelength of X-ray

d: interplanar spacing of crystals,

θ: diffraction angle

n is the order of diffraction

2.9.5.Scanning Electron Microscope :

A scanning electron microscope (SEM) is a type of electron microscope that produces images of a sample by scanning it with a focused beam of electrons. The electrons interact with electrons in the sample, producing various signals that can be detected and that contain information about the sample's surface topography and composition. The electron beam is generally scanned in a raster scan pattern, and the beam's position is combined with the detected signal to produce an image.

- The SEM uses electrons instead of light to form an image.
- A beam of electrons is produced at the top of the microscope by heating of a metallic filament.
- The electron beam follows a vertical path through the column of the microscope. It makes its way through electromagnetic lenses which focus and direct the beam down towards the sample.
- Once it hits the sample, other electrons (backscattered or secondary) are ejected from the sample. Detectors collect the secondary or backscattered electrons, and convert them to a signal that is sent to a viewing screen. SEM can achieve resolution better than 1 nanometer.

CHAPTER-3

Result and Discussion

3.Result and Discussion

3.1. Phase confirmation by x-ray diffraction analysis

Phase analysis was studied using the x-ray diffractogram which is obtained by scanning pelletalized samples in a continuous mode from 20^0-80^0 with a scanning rate of 2^0/minute. The result shows well resolved sharp peaks corresponding to the BSCCO phase. Indexing is done by matching the obtained result with the JCPDS data. The major peaks corresponds to the BSCCO 2212 phase. Besides these prominent peaks, there are some additional peaks corresponding to BSCCO-2223 phase, for Gd doped samples.

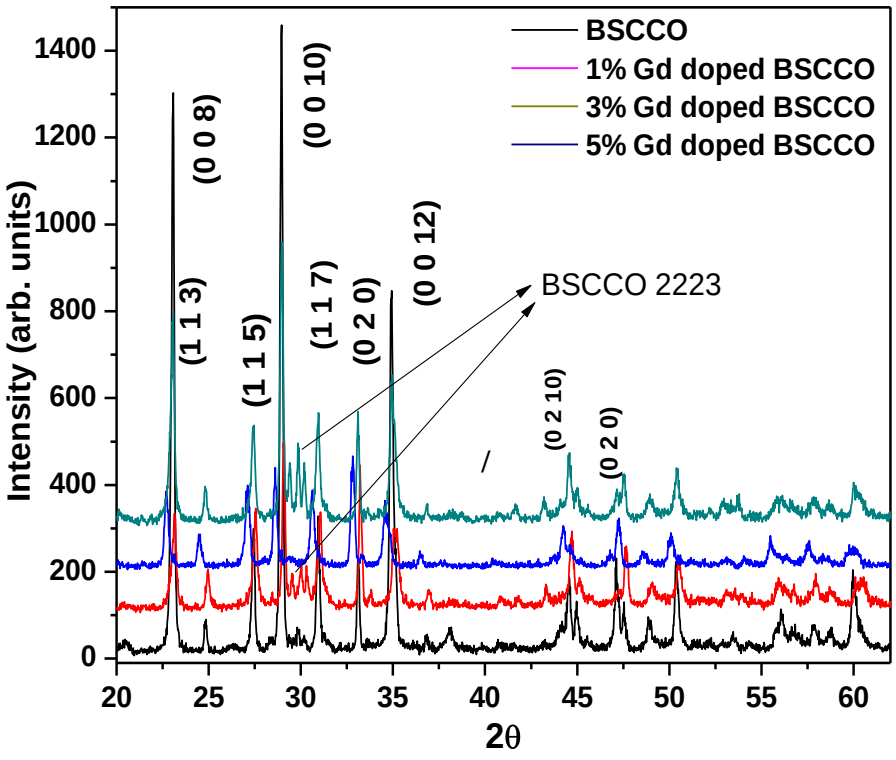

Fig.17. X-ray diffractogram of BSCCO along with 1%, 3% and 5% Gd doped BSCCO. The numerals inside bracket are Miller indices of corresponding planes.

3.2. Scanning Electron Microscopy (SEM):

Microstructural features were studied using SEM. The SEM images of all the samples (BSCCO, 1%, 5% Gd doped BSCCO) having magnification of ×1500. The grain morphology shows clear and flaky grains with layered growth, typical of BSCCO 2212. As the Gd content increases, the flaky nature of the grains gradually disappears with decreasing grain size and increasing porosity.

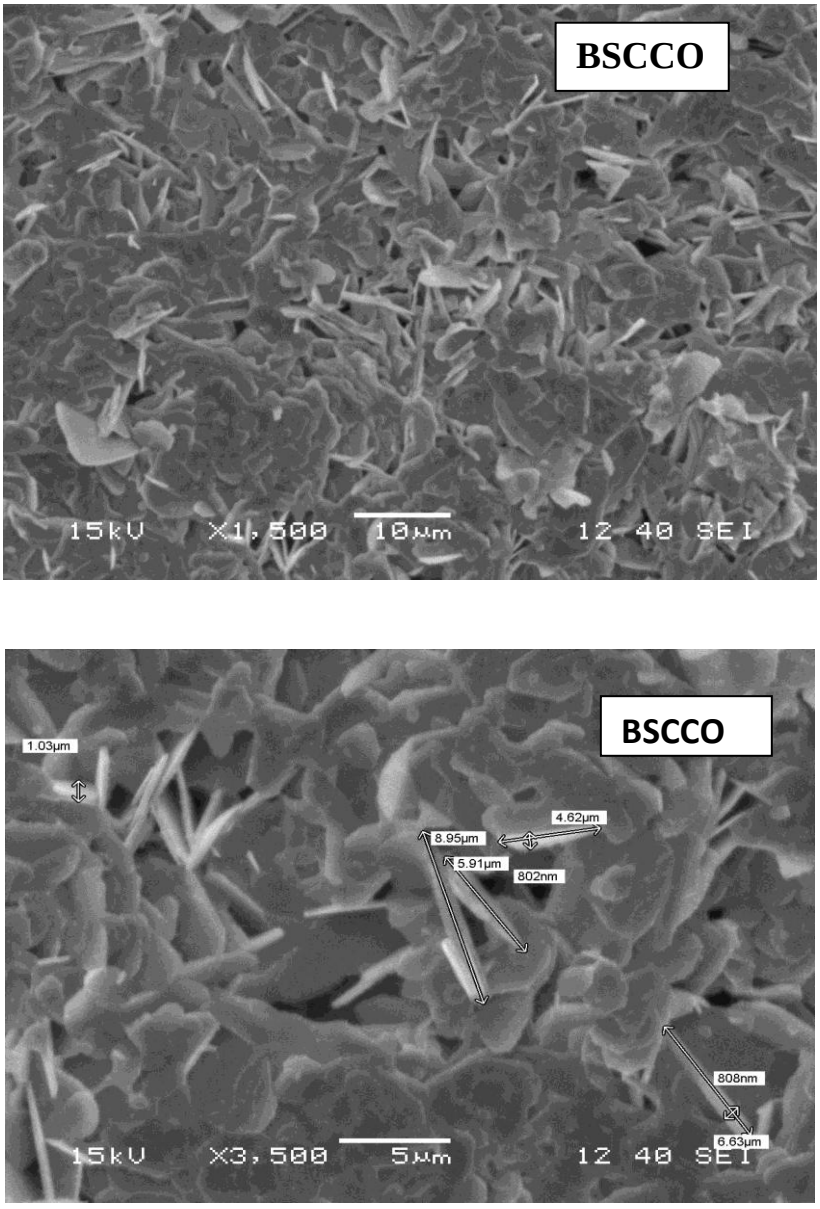

Fig. 18 (a)

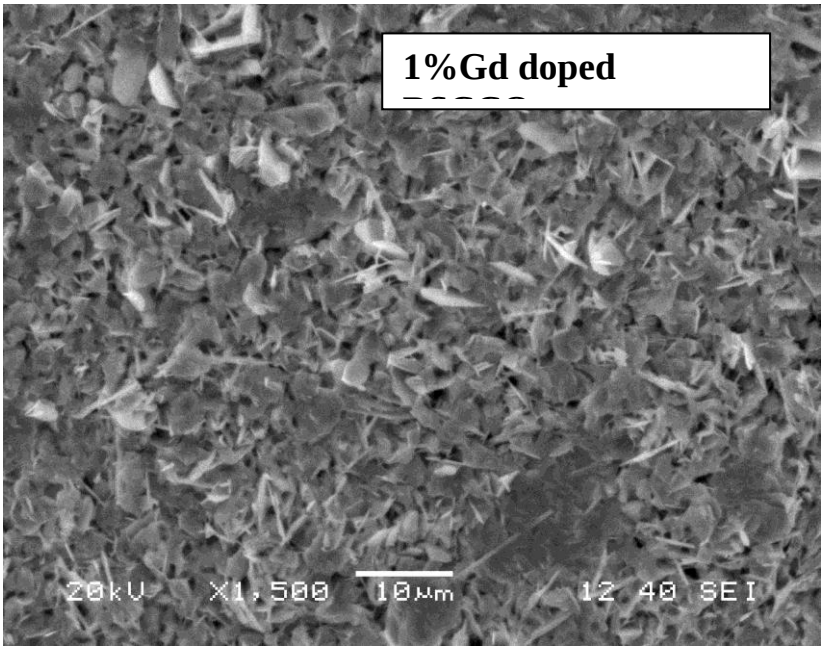

Fig 18(b)

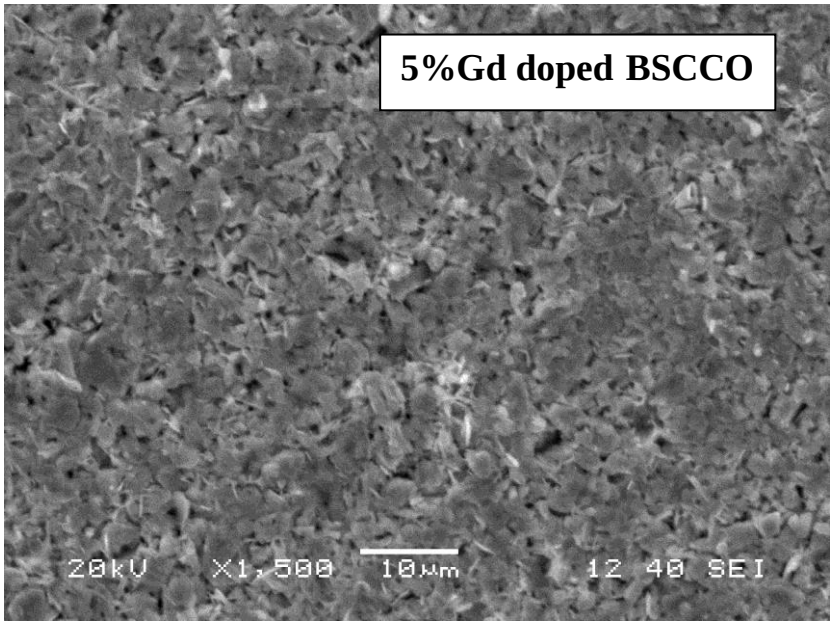

Fig 18(c)

Fig.18(a,b,c): SEM images of BSCCO, 1% and 5%, Gd doped BSCCO shows the variation of microstructure as the doping concentration is increasing in magnification of ×1500

3.3. R-T Measurement:

The R-T measurement of all samples is carried out using four probe arrangement. The temperature dependent resistivity was measured using standard four probe technique with a nanovoltmeter (Keithely 2182), Current source (Keithley 2161) and temperature controller. For R-T measurements, the electrical contacts on the sample were made over the surface of the pellet using silver paste. After the complete drying of the paste the sample which was held over the cryocooler head made closed by putting the shrouds and vacuum is made so as to avoid condensation of air while low temperature. After evacuating, the crycooler started and gradually low temperature is achieved. In this instrument temperature as low as upto 10K can be achieved. To obtain the true voltage from the sample, the measurement is done for both positive & negative currents, which minimizes the thermoelectric voltage. All the data were recorded on the computer screen which is previously programmed using "Lab View" software.

The temperature dependence of resistivity for all the samples is shown in the figure as normalized resistivity with respect to 273K, ρ/ρ_{273} .The behavior of BSCCO is almost linear as the sample is cooled from room temperature. Transition to superconducting state begins at the onset temperature $T_{c\text{-onset}}$ = 84.76K and is complete at T_{c0} = 70.16K. The mean field transition temperature "T_c" is obtained from the derivative plot as shown in figure.

The normal region resistivity for Gd doped BSCCO is much more linear as compared to its undoped counterpart. Also the transition temperatures shift to lower values for all the Gd doped samples. Initially the T_c's decreases for 1% Gd doped sample and for 3% & 5% doped samples, it increases, but still below the parent BSCCO. This increase in T_c, may due to the appearance of BSCCO-2223 phase for Gd-doped samples, as seen in x-ray diffraction results. Also one can see that the transition width ($T_{c\text{-onset}} - T_{c0}$) increases with Gd-doping in BSCCO, indicating the doping induced disorder in the sample. This is in support of the SEM results, which shows the destruction of flaky nature of BSCCO and creation of more porosity, on doping with Gd.

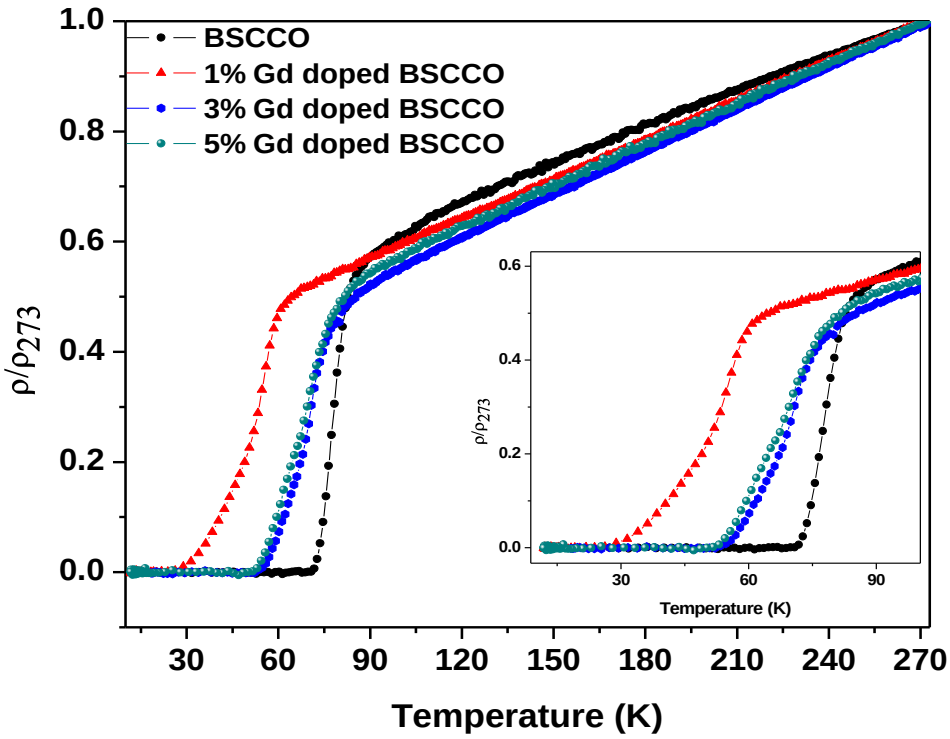

Fig.19. Temperature dependence of resistivity normalized w.r.t. 273K value is shown for BSCCO and 1%, 3%, 5% Gd doped BSCCO. The inset shows the magnified view of the same near the transition temperatures.

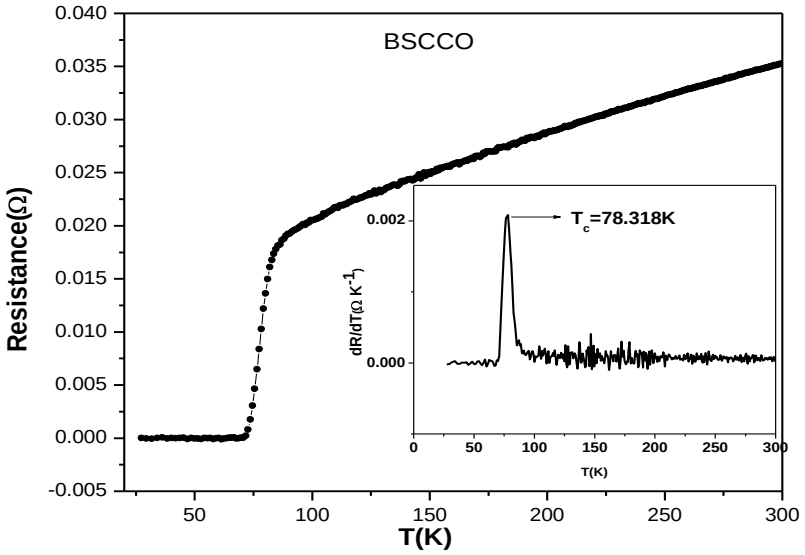
BSCCO
Resistance(Ω)
T(K)
T_c=78.318K
dR/dT(Ω K^{-1})

Fig.20

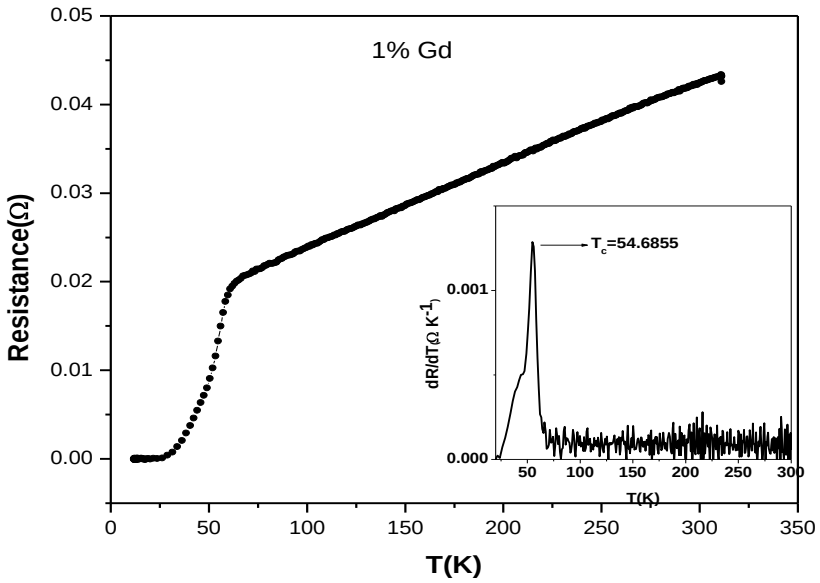
1% Gd
Resistance(Ω)
T(K)
T_c=54.6855
dR/dT(Ω K^{-1})

Fig.21

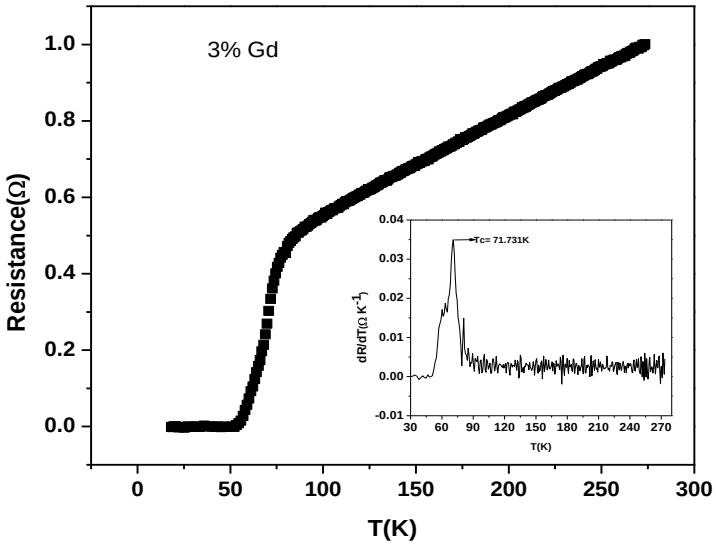

Fig.22

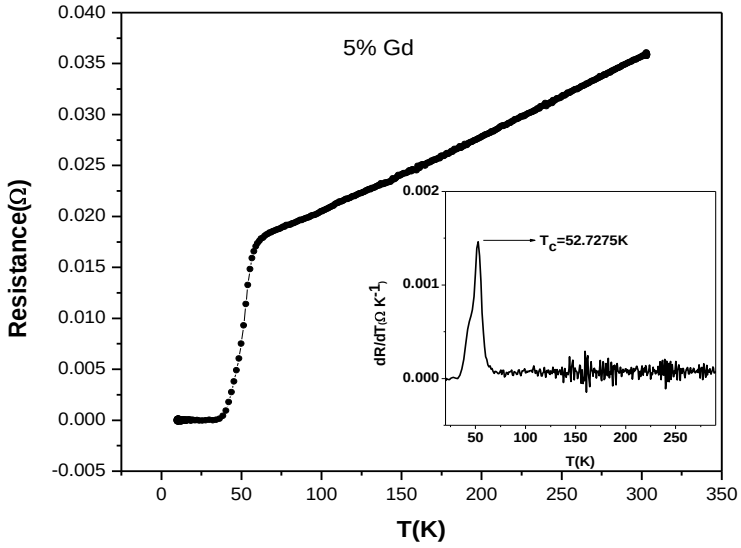

Fig.23

Fig.20, Fig.21, Fig.22, Fig.23: Resistivity(R)-Temperature(T) measurement of Pure BSCCO, 1%, 3%, 5% Gd doped BSCCO respectively. The inset shows the plots of dR/dT against temperature (T) showing the mean field transition temperature T_c by an arrow.

From the peak of derivative plot one obtains the mean field transition temperature Tc, the temperature at which maximum slope change is occurring. $T_{c\text{-}onset}$,is the temperature from which the sample starts to become superconductor where as T_{c0} is the temperature at which the resistance completely becomes zero.

Type of sample	**$T_{c\ onset}$(K)**	**T_{c0}(K)**	**T_c(K)**
Undoped BSCCO	84.76	70.16	71.31
1%Gd doped BSCCO	61.95	24	64.88
3% Gd doped BSCCO	78.09	49.37	71.73
5% Gd doped BSCCO	58.97	48.52	62.72

3.4. I-V Measurements

The critical current density J_c is obtained from the critical current and cross sectional area measurements as per the formula $J_c = I_c/A$. From the I-V plots obtained, the critical current can be measured i.e. the point from which voltage value increase. This measurement is obtained for constant temperature value at a 5K temperature interval. After obtaining the critical current density J_c, it is then fitted to

$$\mathbf{J_c(T) = J_c(0)\ (1-T/T_c)^n}$$

The exponent 'n' takes the values depending on the type of Josephson junction. The value of n = 2 for superconductor–normal metal–superconductor (SNS) junction, and n = 1 for superconductor–insulator–superconductor (SIS) junction. The value $1 < n < 2$ indicates the superconductor–insulator–normal metal-superconductor (SIS) junction.

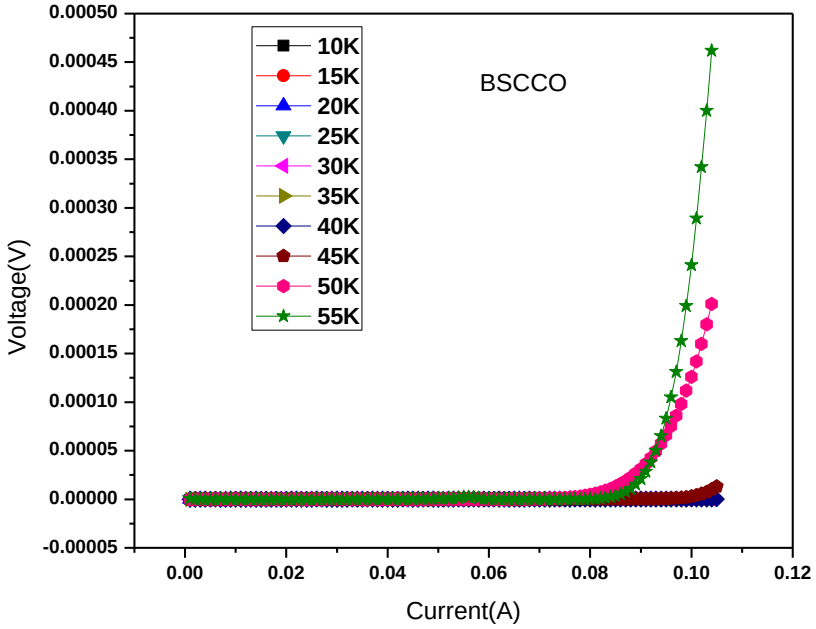

Fig.24: Current (I) - Voltage(V) curves of BSCCO, done by varying current and consequently measuring the voltage by nanovoltmeter, measured at various temperature of 10 K, 15K, 20 K, 25K, 30 K,35K, 40 K, 45K, 50 K, 55K.

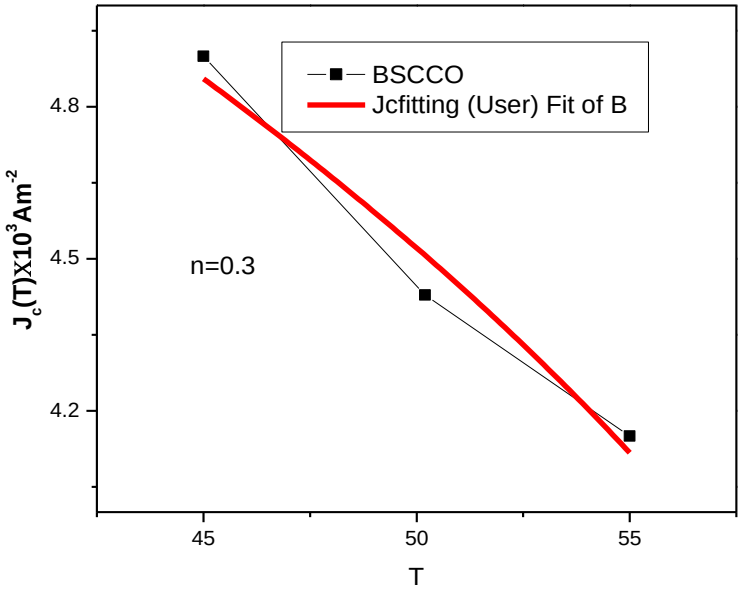

Fig.25: Critical current density (J_c) as a function of temperature -plotted against temperature(T) for BSCCO which is fitted with the equation

$$J_c(T) = J_c(0)\,(1-T/T_c)^n$$

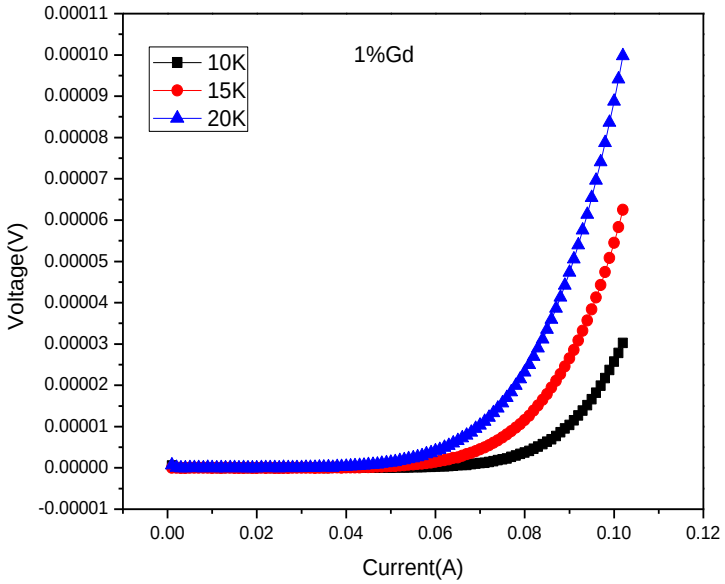

Fig.26: Current (I)-Voltage(V) curves of 1% Gd doped BSCCO, done by varying current and consequently measuring the voltage by nanovoltmeter, measured at various temperatures of 10 K, 15K, 20 K.

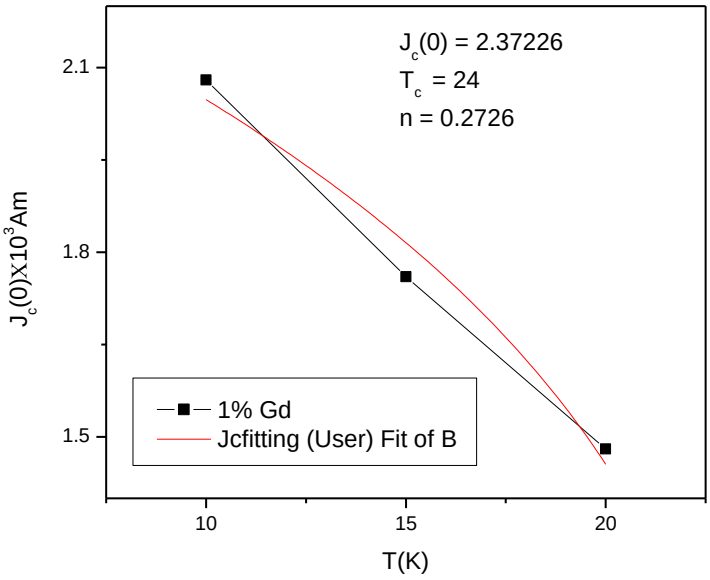

Fig.27: critical current density (J_c) as a function of temp.-plotted against temperature(T) for 1% Gd doped BSCCO which is fitted with the equation

$$J_c(T) = J_c(0)\,(1-T/T_c)^n$$

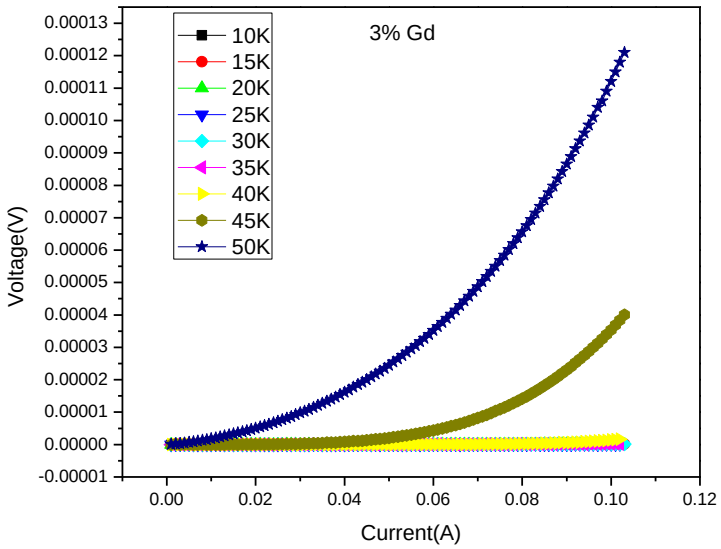

Fig.28: Current (I) - Voltage(V) curves of 3% Gd doped BSCCO, done by varying current and consequently measuring the voltage by nanovoltmeter, measured at various temperature of 10 K, 15K, 20 K, 25K, 30 K,35K, 40 K, 45K, 50 K.

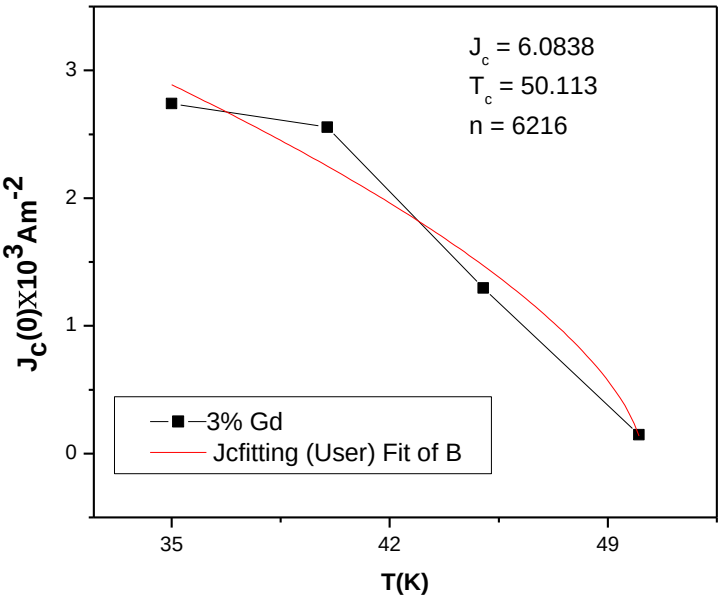

Fig.29: critical current density (J_c) as a function of temperature -plotted against temperature(T) for 3% Gd doped BSCCO which is fitted with the equation

$$J_c(T) = J_c(0)\,(1-T/T_c)^n$$

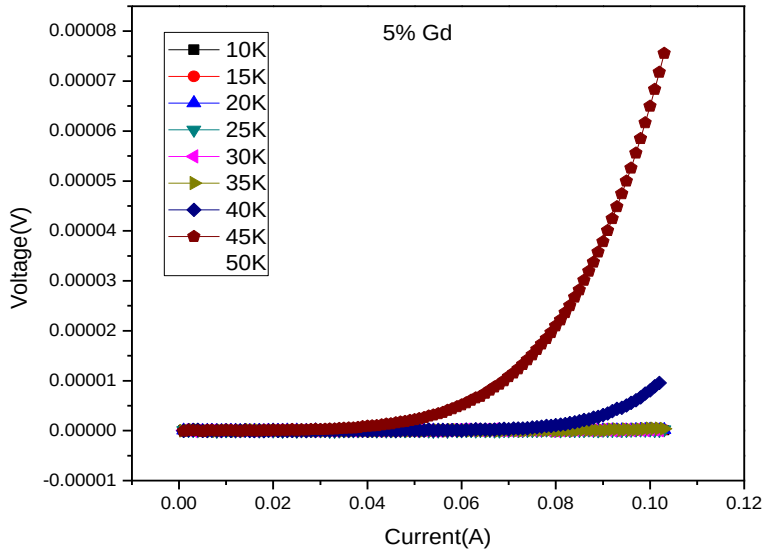

Fig.30: Current (I) - Voltage(V) curves of 5% Gd doped BSCCO, done by varying current and consequently measuring the voltage by nanovoltmeter, measured at various temperature of 10 K, 15K, 20 K, 25K, 30 K,35K, 40 K, 45K, 50 K.

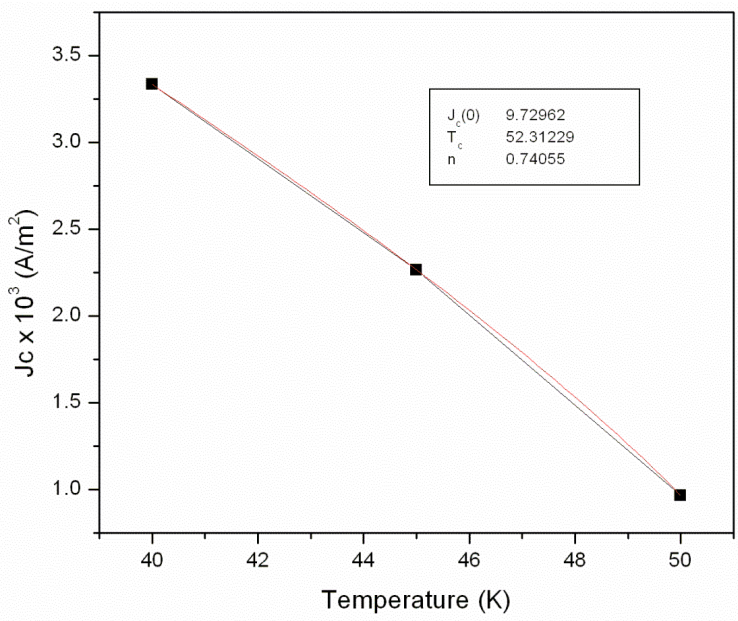

Fig.31: critical current density (J_c) as a function of temperature -plotted against temperature(T) for 5% Gd doped BSCCO which is fitted with the equation

$$J_c(T) = J_c(0)\,(1\text{-}T/T_c)^n$$

Conc.of Gd	J_c (0) in Am^{-2}	n	T_c
0% (BSCCO)	6.684	0.3	70.16
1%	2.37226	0.2726	24
3%	6.0838	0.6216	49.37
5%	9.73	0.74055	52.31

Here as "n" value is gradually increasing which state that the insulating property is increasing by increasing doping concentration and it is approaching towards SIS junction because for Superconductor-insulator-superconductor junction n=1.

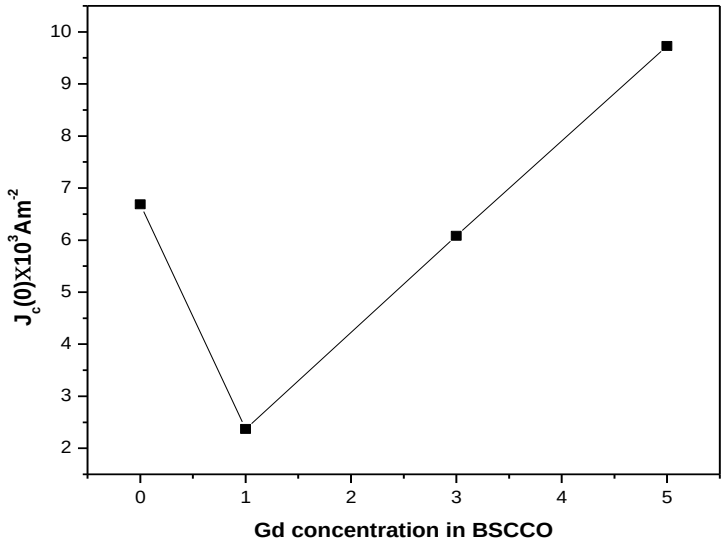

Fig.32. critical current density (J_c) plotted against different concentration of Gd in BSCCO-2212.

The plot shows J_c value after being decreased with respect to parent BSCCO value for 1% Gd doping, there is a gradual increase in J_c for increasing concentrations of Gd doping.

CHAPTER-4

Conclusion

4.1.Conclusion:

The successful preparation of lead free BSCCO-2212 phase is done by solid state reaction rout. Again it's been doped with Gd of different concentrations (1%, 3%, 5%) following the same methodology. From the XRD analysis, BSCCO phase formation is confirmed. This shows well distinguished sharp peaks corresponding to the BSCCO phase. Additional peaks are seen on doping the BSCCO with Gd. The additional peaks are in agreement with that of BSCCO-2223 phase, as per JCPDS data. The major peaks of Gd-doped BSCCO still corresponds to the BSCCO 2212 phase.

- ✓ So this confirms the appearance of additional BSCCO-2223 phase as the doping concentration is increasing w.r.t. the parent BSCCO.
- ✓ From the SEM graphs confirms flaky nature of BSCCO. As the concentration increases the flaky nature diminishes and porosity increases.
- ✓ From the R-T measurement the superconducting transition temperature is found out and the derivative plot gives the mean field transition temperature.
- ✓ The normal region resistivity for Gd doped BSCCO is much more linear as compared to its undoped counterpart. Also the transition temperatures shift to lower values for all the Gd doped samples. Initially the T_c's decreases for 1% Gd doped sample and for 3% & 5% doped samples, it increases, but below the parent BSCCO. This increase in T_c, may due to the appearance of BSCCO-2223 phase for Gd-doped samples, as seen in x-ray diffraction results.
- ✓ Also one can see that the transition width ($T_{c\text{-onset}} - T_{c0}$) increases with Gd-doping in BSCCO, indicating the doping induced disorder in the sample. This is in support of the SEM results, which shows the destruction of flaky nature of BSCCO and creation of more porosity, on doping with Gd.
- ✓ The critical current density J_c is obtained from the critical current and cross sectional area measurements as per the formula $J_c = I_c/A$. Current (I) - Voltage(V) curves, done by varying current and consequently measuring the voltage by nanovoltmeter, measured at various temperature, which gives the I_c value and so as J_c is obtained by dividing with the cross-sectional area of the sample. After obtaining the critical current density J_c, it is then fitted to

$$J_c(T) = J_c(0)\,(1-T/T_c)^n$$

where ‘n’ represents the type of Joshephson junction.

- ✓ Here “n” value is gradually increasing towards ‘1’ with increased concentration of Gd doping, which state that the insulating property is increasing by increasing doping concentration and it is approaching towards SIS junction because for Superconductor-insulator-superconductor junction, n=1.
- ✓ The variation of critical current density (J_c) with increasing concentrations of Gd in BSCCO-2212 plot shows that, the Jc value after being decreased w.r.t. parent BSCCO for 1% Gd doping, there is a gradual increase in Jc for 3% and 5% of Gd doping. This concludes that this doping is acting as a pinning center.

4.2.Bibliography:

[1] Tinkham, Introduction to Superconductivity, 2nd Edition, Dover publication.

[2] Elementary Solid State Physics, Ali and Omar, Pearson Publication.

[3] Charles Kittel, Introduction to solid state physics, Seventh edition, Wiley India, 2004

[4] S.Acharya, A.K.Biswal, J.Ray, P.N.Vishwakarma, Journal of Applied Physics, 112, 053916 (2012).

[5] D.H. Galvan, J. supercond. Nov. Magn., **21**, 271 (2008).

[6] BSCCO www.wikipedia.com

[7] Rusland Prozorov, Tanya Prozorov and Alexey Snezhko,Superconducting Nanocomposites, IEEE Transactions on Applied Superconductivity, **15**, (2005).

[8] Shi Zhixiang, Ji Helin, Zhang Yitong, Jin Xin, Xu Xiaonong, Ding Shiying and Yao Xixian, Acta Physica Sinica (Overseas Edition), **3**, P124 (1994)

[9] Y.Sun, Y.Ding, J.C.Zhuang, L.J.Cui, X.P.Yuan, Z.X.Shi, Z.A.Ren, The critical current of SC, Low Temperature Physics, **27**, (2001).

[10] Alexey Snezhko, Tanya Prozrov, Ruslan Prozrov, University of South Carolina,Coulombia, **28,** SC 29208 (2004).

[11] R P Aloysius,P Guruswamy and U Syamaprasad,Institute of Physics Publishing,Supercond.sci.Technol.**18,** L23-L28 (2005).

[12] L.Dimess and R.Masini, Physica, M.L. Cavinato, D.Fiorani and A.M.Testa, Japanese Journal of Applied Physics **C203** 403-410 (1992).

[13] J .M. Tarascon, Phys. Rev. B, **37**, 7458 (1988).

[14] T.Di.Luccio, Phys. Rev. B. **67**, 092504 (2003).

[15] N.A.Prytkova And Zh.M.Tomilo,Acad. Of science,Minsk, IEEE Transactions on Applied Superconductivity, **9,** 1051-8223 (1999).

[16] A.C.Meltzow, Physica, **C302,** 207-214 (1998).

[17] R.Ramesh, M.S.Hegde.J. Appl. Phys., **66**, 10 (1989).

[18] S. Vinu, P.V. Shabana, R. Shabnam, A. Biju, P. Guruswamy, U. Syamaprasad, Solid State Sci. **104,** 043905 (2008).

[19] D R Mishra,Pramana Journal of physics,Indian Academy of Sciences,**70,** 535-541 (2008).

[20] A Biju, P M Sarun, R P Aloysius and U Syamaprasad , Superconductor Science and Technology, **19**, 0953-2048 (2006).

[21] B.A. Albiss, I.M. Obaidat , M. Gharaibeh, H. Ghamlouche , S.M. Obeidat, Solid State Commun.**, 150**, 1542-1547 (2010).

[22] R H Patel, Supercond. Sci. Technol. **18**, 317-324 (2005)**.**